

## Evolution of Curie-Weiss behavior and cluster formation temperatures in Ru-doped $\text{Sm}_{0.55}\text{Sr}_{0.45}\text{MnO}_3$ manganites

M. M. Saber,<sup>\*</sup> M. Egilmez, A. I. Mansour, I. Fan, K. H. Chow, and J. Jung<sup>†</sup>

*Department of Physics, University of Alberta, Edmonton, Canada T6G 2G7*

(Received 3 February 2010; revised manuscript received 9 August 2010; published 1 November 2010)

We investigated magnetotransport properties, such as the clustering temperature  $T^*$ ,  $T_C$ , magnetoresistance, and the resistivity of  $\text{Sm}_{0.55}\text{Sr}_{0.45}\text{MnO}_3$  manganite (which exhibits a non-Curie-Weiss (CW) behavior, resulting from the multiphase competition and coexistence), and their evolution due to ruthenium doping on the Mn-ion site ( $B$ -site). These results have been compared with the predictions of a model of a system of two competing states in the presence of quenched disorder. Ru doping, which causes an interplay between the promotion of the long-range metallic ferromagnetic phase and the  $\text{Mn}^{3+}\text{-Mn}^{4+}$  ions clustering, results in a suppression of the deviation from the Curie-Weiss law in  $H/M(T)$ , which is accompanied by an increase in  $T_C$ , a decrease in the resistivity and a reduction in the magnetoresistance. However  $T^*$  is little affected by the doping.

DOI: [10.1103/PhysRevB.82.172401](https://doi.org/10.1103/PhysRevB.82.172401)

PACS number(s): 75.47.Lx, 75.47.Gk, 75.60.Ej, 71.27.+a

An upward deviation from the Curie-Weiss (CW) law  $\chi^{-1}=(T-\theta_p)/C$ , where  $\chi^{-1}$ ,  $C$ , and  $\theta_p$  are reciprocal magnetic susceptibility, Curie constant, and the paramagnetic Curie temperature (the Curie-Weiss temperature), respectively, has been observed in  $\text{Sm}_{1-y}\text{Sr}_y\text{MnO}_3$  (SSMO) manganites for compositions  $y=0.35-0.50$  close to half doping.<sup>1-3</sup> This property is governed by the formation of charge ordered/orbital ordered (CO/OO) phases in the paramagnetic (PM) state,<sup>1,4,5</sup> and has been attributed to the beginning of the strong competition between the ferromagnetic (FM) and CO/OO phases.<sup>6</sup> This has been supported by the small-angle neutron scattering and muon spin relaxation ( $\mu\text{SR}$ ) studies of these compositions, which revealed that its PM ground state consists of nanosize FM clusters incorporated within a short-range CO/OO matrix.<sup>6</sup> The colossal magnetoresistance (CMR) effect observed in SSMO stems from the percolation of these FM clusters. The SSMO system and its underlying magnetic properties are therefore good candidates for studies of the competition between ordered phases caused by quenched disorder.

A model of the competition between ordered states separated by a first-order transition, due to quenched disorder in CMR manganites, has been proposed by Burgy *et al.*<sup>7</sup> They introduced an important parameter, the temperature scale  $T^*$  at which clusters form in the regime of competing orders above the ordering temperature  $T_O$ . For CMR manganites, such as the SSMO system,  $T^*$  corresponds to the temperature below which  $\chi^{-1}$  starts to deviate from the CW law, and  $T_O$  coincides with  $T_C$ . The first-order transition becomes continuous when disorder is sufficiently large. This creates an intermediate region ( $T_O \leq T \leq T^*$ ) where FM and CO clusters coexist in a PM matrix (see Fig. 1 in Ref. 7).  $T_O$ , which increases sharply with an increasing magnetic coupling, is strongly influenced by the magnitude of disorder. On the other hand,  $T^*$  increases with an increasing coupling too but more slowly than  $T_O$ . The dependence of  $T_C$  and  $T^*$  on an increasing magnetic coupling agrees qualitatively with experiments performed on  $A$ -site ( $RE$ -site) doped manganites, such as  $RE_{0.55}\text{Sr}_{0.45}\text{MnO}_3$  which show that both temperatures increase with an increasing tolerance factor.<sup>7</sup>

The question is what happens to these two temperatures

when the quenched disorder is introduced into a CMR manganite by different means, such as doping at the Mn-ion site ( $B$ -site doping). Do the theoretical predictions mentioned above apply also to the  $B$ -site doping induced changes in  $T_C$  and  $T^*$ ? For example, ruthenium (Ru) ion, when substituted for Mn ion in SSMO manganite close to half doping, such as  $\text{Sm}_{0.55}\text{Sr}_{0.45}\text{MnO}_3$  transforms the CO/OO phases in the PM state into the FM phase.<sup>8,9</sup> Consequently, Ru-site doping induced suppression of the charge ordering process manipulates the phase competition between the short-range FM clusters and the CO/OO phase and leads to an increase in  $T_C$ . Therefore, ruthenium is a good candidate for studies of  $T^*$ , its relationship with  $T_C$  due to  $B$ -site doping, and the predictions of the model. The changes in the properties of SSMO due to this doping could be monitored using the measurements of the temperature dependence of the reciprocal susceptibility.

This Brief Report analyzes the effects of Ru substitution at Mn-ion site on  $T^*$ ,  $T_C$ , and the magnetotransport properties of  $\text{Sm}_{0.55}\text{Sr}_{0.45}\text{MnO}_3$ . An increase in  $T_C$  with doping is associated with a decrease in the resistivity and a suppression of the MR but  $T^*$  and metal-insulating transition (MIT) temperature ( $T_{\text{MIT}}$ ) show only a weak dependence on doping. These results are attributed to an interplay between the promotion of the long-range FM phase and the clustering of Mn ions, induced by Ru doping. They are compared with the theoretical predictions of the effects of magnetic coupling and quenched disorder on the phase diagram of manganites by Burgy *et al.*<sup>7</sup>

Samples with the composition  $\text{Sm}_{0.55}\text{Sr}_{0.45}\text{Mn}_{1-x}\text{Ru}_x\text{O}_3$  (SSMRO) for doping levels  $0.00 \leq x \leq 0.10$  were prepared using a standard solid-state reaction technique. The appropriate ratio of  $\text{Sm}_2\text{O}_3$ ,  $\text{SrCO}_3$ ,  $\text{MnO}_2$ , and  $\text{RuO}_2$  was mixed, pressed, and calcined at  $1200^\circ\text{C}$  for 24 h in air. The resultant samples were ground, pressed, and sintered under the same conditions twice. X-ray diffraction has confirmed the phase homogeneity of the SSMRO. They indicate the presence of a single phase upon doping with ruthenium. Scanning electron micrographs (SEMs) showed similar grain structure in samples with doping levels up to  $x=0.05$ ; however, it revealed much higher grain boundary density in the sample with  $x=0.10$ .

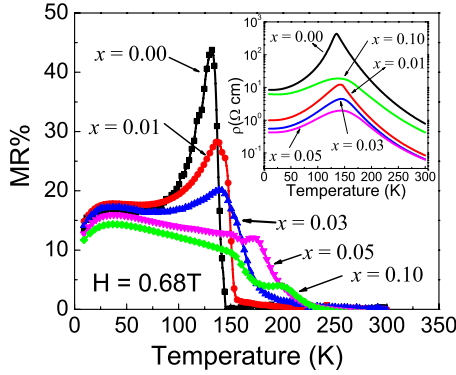


FIG. 1. (Color online) Temperature dependence of the MR at 0.68 T for SSMRO at doping levels  $x=0, 0.01, 0.03, 0.05$ , and  $0.10$ . Inset: temperature dependence of the resistivity at the MIT for all samples.

The temperature dependence of the resistivity and the magnetoresistivity,  $MR = \{[\rho(0) - \rho(H)] / \rho(0)\}$ , where  $\rho(H)$  and  $\rho(0)$  are the resistivity in an applied field of 0.68 T and in a zero field, respectively, was measured over a temperature range of 10–300 K using the standard four-probe method. The temperature dependence of the magnetization over the same temperature range was measured with a superconducting quantum interference device magnetometer (Quantum Design) using the following procedure: the samples were first cooled down from high temperatures ( $T > T_C$ ) to the temperature of interest in a magnetic field [field cooling (FC)]. Then the measurement of the magnetization was performed during warming in the presence of the same field.

The temperature dependence of the resistivity  $\rho$  measured for Ru-doping levels  $x$  between 0.00 and 0.1 are shown in the inset of Fig. 1. It shows a continuous drop of the resistivity at the MIT and an increase in the MIT temperature  $T_{MIT}$  with an increasing Ru doping for doping levels  $x \leq 0.05$ . The resistivity of a sample with  $x=0.1$  is higher than that of all doped samples. This could be attributed to higher density of grain boundaries in this sample, as observed by SEM. The width of the resistivity peak and the magnitude of the residual resistivity ratio ( $\rho_0 / \rho_{MIT}$ ) at 10 K increase with an increasing  $x$ . The temperature dependence of the MR for an undoped  $\text{Sm}_{0.55}\text{Sr}_{0.45}\text{MnO}_3$  (see Fig. 1) shows a peak near the MIT. At lower temperatures the observed magnetoresistance is believed to originate from the tunnel magnetoresistance through the grain boundaries.<sup>10</sup> Ru-doping results in a gradual overall decrease in the MR with an increasing  $x$ . In particular, a peak at temperatures close to the MIT seen in the undoped SSMO sample was observed to broaden and diminish with an increasing  $x$  in the SSMRO samples.

The measurement of the temperature dependence of the FC magnetization at 0.68 T [see Fig. 2(a)], shows an increase in  $T_C$  with an increasing doping level, in agreement with previous studies.<sup>11</sup> The Curie temperature  $T_C$  was estimated using the gradient method, i.e., it is taken as the temperature at which the change in the gradient of the magnetization is maximum. All samples exhibit magnetic transitions at temperatures significantly higher than the MIT temperature [see the inset of Fig. 2(a)].

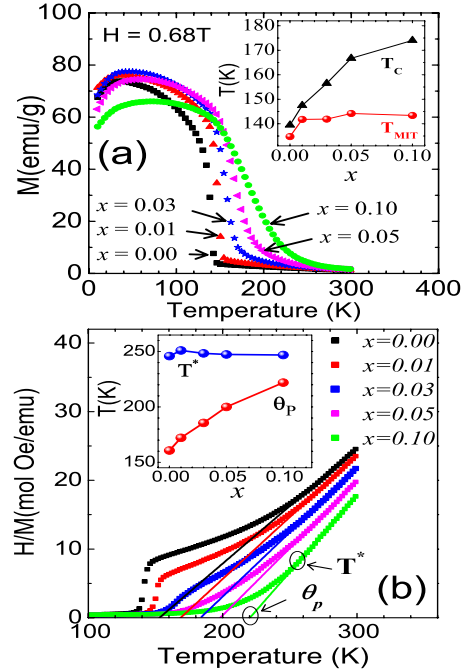


FIG. 2. (Color online) (a) Temperature dependence of the magnetization of SSMRO for doping levels  $x$  between 0 and 0.10. Inset: dependence of  $T_C$  and  $T_{MIT}$  on  $x$ . (b) The corresponding temperature dependence of the inverse susceptibility  $H/M$ . The solid lines are the fits to the equation:  $H/M = (T - \theta_p) / C$ , where  $\theta_p$  is the paramagnetic Curie temperature. Inset: dependence of  $T^*$  and  $\theta_p$  on  $x$ .

The temperature dependence of  $H/M$  for the SSMO and SSMRO is presented in Fig. 2(b). The data for the undoped SSMO show a clear deviation from the CW law starting approximately below 250 K, well above  $T_C$  for this composition. The  $T^*$  marks the temperature below which a clear upturn deviation from the CW law in the PM state is observed. The inset of Fig. 2(b) shows the discrepancy between  $T^*$  and the paramagnetic Curie temperature  $\theta_p$ . As the Ru content increases, the difference between  $T^*$  and  $\theta_p$  decreases.

Below, we analyze the effect of ruthenium at the Mn-ion site on the properties of SSMO. We concentrate on the dependence of  $T^*$  and  $T_C$  on  $x$ , and discuss it in terms of the theoretical predictions of Burgy *et al.* model.<sup>7</sup>

Ru has extended  $4d$  orbitals which have greater overlap and hybridization with O: $2p$  orbitals than those of  $3d$  ions. This causes a wide bandwidth in Ru oxide, resulting in a more metallic behavior.<sup>12</sup> Ru doping on the Mn site in manganites causes a decrease in the Mn valence and an increase in the concentration of  $\text{Mn}^{3+}$  ions since it exists as a pentavalent ( $\text{Ru}^{5+}$ ) or tetravalent cation ( $\text{Ru}^{4+}$ ) in the  $\text{Mn}^{3+}\text{-O-Mn}^{4+}$  network.<sup>12</sup> It increases the effective carrier density on the Mn sites through the charge neutrality requirement.<sup>8,9</sup> These effects contribute to a decrease in the resistivity at the MIT with an increasing  $x$ , as was observed for the doping level  $x$  up to 0.05 (see Fig. 1). On the other hand, small effect of Ru doping on the magnitude of  $T_{MIT}$  [see the inset of Fig. 2(a)] could be the result of the superexchange FM interaction which can occur between  $\text{Mn}^{3+}$  and  $\text{Ru}^{5+}(\text{Ru}^{4+})$ . Such an interaction produces ferromagnetic insulating phase which

could limit the increase in  $T_{\text{MIT}}$  with Ru doping, according to Ref. 13. An increase in the width of the resistivity peak and the magnitude of the residual resistivity ratio ( $\rho_0/\rho_{\text{MIT}}$ ) at 10 K with an increasing  $x$  (see the inset in Fig. 1) is consistent with an increasing amount of disorder with doping.<sup>14–16</sup> An increasing  $x$  leads also to a suppression of the MR peak in the vicinity of the MIT (Fig. 1).

As mentioned in the introduction an increase in  $T_C$  due to ruthenium doping occurs in  $\text{Sm}_{1-y}\text{Sr}_y\text{Mn}_{1-x}\text{Ru}_x\text{O}_3$  for SSMO compositions  $y$  between 0.35 and 0.60.<sup>11</sup> At these compositions the formation of the CO/OO phase was verified using Raman scattering,<sup>5</sup> optical conductivity,<sup>17</sup> and x-ray diffuse scattering.<sup>5</sup>

An increase in  $T_C$  with an increasing concentration of ruthenium is related to transformation of the CO/OO phase into the FMM phase in the temperature range  $T_C \leq T \leq T^*$ .<sup>11</sup> Ru doping causes the long-range FMM phase to form preferentially at the expense of the CO/OO phase; this preferential formation of the FMM phase is attributed to the existence of a random distribution of Ru ions which participate in destroying the AFM ordering in the CO/OO clusters.<sup>8,9</sup>

The evolution of the Curie-Weiss behavior with an increasing Ru doping allowed us to gain additional insight into the magnetic interactions present in these materials. We calculated the molecular field constant  $\lambda$  ( $\lambda = \theta_p/C$ ) and the effective paramagnetic moment  $P_{\text{eff}}$  (from the Curie constant  $C = \mu_B^2 P_{\text{eff}}^2 N_A / 3k_B$ ) using the reciprocal susceptibility data. This was done for two temperature regimes: above  $T^*$  and below  $T^*$  (down to  $T^* - 15$  K). The dependence of  $\lambda$  and  $P_{\text{eff}}$  on the Ru-doping level  $x$  is shown in Fig. 3.  $\lambda$  increases continuously with Ru doping both above and below  $T^*$  showing the enhanced FM correlation with Ru doping. On the other hand,  $P_{\text{eff}}$  is the largest in the undoped sample and higher than the expected value of 4.47 for free Mn moments. This suggests that in this sample the strong FM coupling between  $\text{Mn}^{+3}$  and  $\text{Mn}^{+4}$  ions causes a local accumulation of  $\text{Mn}^{+3}$  around  $\text{Mn}^{+4}$  in large clusters, in the PM state above and below  $T^*$ .<sup>2,18</sup>  $P_{\text{eff}}$  decreases slightly with increasing  $x$  (it drops by about 10–15 % in SSMRO with  $x=0.1$ ), suggesting that the size of these clusters is reduced by Ru doping.<sup>2</sup> The reduction in MR and a relatively small change in  $T_{\text{MIT}}$  could be then explained by the absence of percolative pathways between the FM clusters, created by the Ru doping in the CO AFM matrix. This indicates an interplay between the promotion of the long-range FMM phase and the  $\text{Mn}^{+3}$ - $\text{Mn}^{+4}$  ions clustering, induced by Ru doping.

A continuous increase in  $\lambda$  with an increasing Ru doping both above and below  $T^*$  confirms the correlation between the doping and the increase in FM coupling in SSMRO samples. Such a correlation enables one to compare the results shown in the inset of Fig. 2(b) with the phase diagram obtained using Burgy's *et al.* model simulations of a system of two competing states.<sup>7</sup> The model predicts an increase in  $T_C$  and a suppression of clustering temperature range ( $T^* - \theta_p$ ) with an increasing magnetic coupling. These predic-

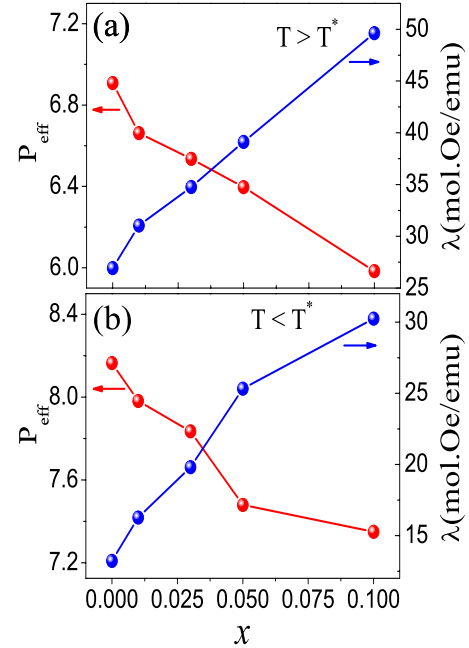


FIG. 3. (Color online) The effective paramagnetic moment  $P_{\text{eff}}$  and molecular field constant  $\lambda$  (a) above  $T^*$  and (b) below  $T^*$  for doping levels  $x$  between 0 and 0.10.

tions agree qualitatively with the results shown in Fig. 2(b) assuming a small increase in disorder with doping. Furthermore, the model suggests a reduction in the resistivity peak with an increasing ordering temperature  $T_C$ , which also agrees with our results. However, a gradual increase in  $T^*$  with an increasing magnetic coupling, predicted by the model, is not consistent with our results where  $T^*$  depends only weakly on doping. A possible reason is that the calculated  $T^*$  refers to the idealized clean (disorder-free) system while the experimental  $T^*$  could be affected by a number of sources of disorder in the material. For example, the  $T^*$  that we infer at  $x=0$  is already affected by  $A$ -site disorder ( $\sigma_A$ ), and with further  $B$ -site substitution  $T^*$  depends on both  $\sigma_A$  and  $B$ -site disorder.

In summary, we analyzed the effects of Ru doping at the Mn site in  $\text{Sm}_{0.55}\text{Sr}_{0.45}\text{Mn}_{1-x}\text{Ru}_x\text{O}_3$  manganite on its magnetotransport properties. In particular, we investigated changes in  $T^*$ ,  $T_C$ , MR, and the resistivity of this manganite. Ru doping promotes the FM phase but seems to reduce the size of the  $\text{Mn}^{+3}$ - $\text{Mn}^{+4}$  ions clusters, resulting in an increase in  $T_C$ , suppression of the resistivity and the CMR properties, but it has a little effect on  $T^*$ . The experimental results have been compared with the predictions of a model of a system of two competing states.<sup>7</sup> Qualitative agreement was found in the behavior of  $T_C$ , a clustering temperature range ( $T^* - \theta_p$ ), and the resistivity at the MIT. The model however does not predict the small changes in  $T^*$  due to Ru doping.

We are grateful to E. Dagotto and P. Majumdar for useful comments. This work was supported by NSERC.

\*melsayed@phys.ualberta.ca

†jung@phys.ualberta.ca

- <sup>1</sup>A. Hassen and P. Mandal, *J. Appl. Phys.* **101**, 113917 (2007).
- <sup>2</sup>R. P. Borges, F. Ott, R. M. Thomas, V. Skumryev, J. M. D. Coey, J. I. Arnaud, and L. Ranno, *Phys. Rev. B* **60**, 12847 (1999).
- <sup>3</sup>A. Rebello and R. Mahendiran, *Phys. Rev. B* **93**, 232501 (2008).
- <sup>4</sup>C. Martin, A. Maignan, M. Hervieu, and B. Raveau, *Phys. Rev. B* **60**, 12191 (1999).
- <sup>5</sup>E. Saitoh, Y. Tomioka, T. Kimura, and Y. Tokura, *J. Phys. Soc. Jpn.* **69**, 2403 (2000).
- <sup>6</sup>J. M. De Teresa, M. R. Ibarra, P. Algarabel, L. Morellon, B. Garcia-Landa, C. Marquina, C. Ritter, A. Maignan, C. Martin, B. Raveau, A. Kurbakov, and V. Trounov, *Phys. Rev. B* **65**, 100403(R) (2002).
- <sup>7</sup>J. Burgy, M. Mayr, V. Martin-Mayor, A. Moreo, and E. Dagotto, *Phys. Rev. Lett.* **87**, 277202 (2001).
- <sup>8</sup>X. Chen, S. Dong, K. Wang, J. M. Liu, and E. Dagotto, *Phys. Rev. B* **79**, 024410 (2009).
- <sup>9</sup>K. Pradhan, A. Mukherjee, and P. Majumdar, *EPL* **84**, 37007 (2008).
- <sup>10</sup>H. Y. Hwang, S.-W. Cheong, N. P. Ong, and B. Batlogg, *Phys. Rev. Lett.* **77**, 2041 (1996).
- <sup>11</sup>A. Maignan, C. Martin, M. Hervieu, B. Raveau, and J. Hejtmanek, *J. Appl. Phys.* **89**, 2232 (2001).
- <sup>12</sup>J. S. Kim, D. C. Kim, G. C. McIntosh, S. W. Chu, Y. W. Park, B. J. Kim, Y. C. Kim, A. Maignan, and B. Raveau, *Phys. Rev. B* **66**, 224427 (2002).
- <sup>13</sup>Y. Ying, J. Fan, L. Pi, Z. Qu, W. Wang, B. Hong, S. Tan, and Y. Zhang, *Phys. Rev. B* **74**, 144433 (2006).
- <sup>14</sup>R. Mahesh, R. Mahendiran, A. K. Raychaudhuri, and C. N. R. Rao, *Appl. Phys. Lett.* **68**, 2291 (1996).
- <sup>15</sup>M. Egilmez, Z. Salman, A. I. Mansour, K. H. Chow, and J. Jung, *J. Appl. Phys.* **104**, 093915 (2008).
- <sup>16</sup>A. S. Alexandrov, A. M. Bratkovsky, and V. V. Kabanov, *Phys. Rev. Lett.* **96**, 117003 (2006), and references therein.
- <sup>17</sup>E. Saitoh, Y. Okimoto, Y. Tomioka, T. Katsufuji, and Y. Tokura, *Phys. Rev. B* **60**, 10362 (1999).
- <sup>18</sup>N. Gayathri, A. K. Raychaudhuri, S. K. Tiwary, R. Gundakaram, A. Arulraj, and C. N. R. Rao, *Phys. Rev. B* **56**, 1345 (1997).